

Reactive Intermediates in the Photolytic Decarbonylation of the Acyl Complex $(\eta^5\text{-C}_5\text{H}_5)\text{Fe}(\text{CO})_2(\text{COCH}_3)$ As Studied by Time-Resolved Infrared Spectral Techniques

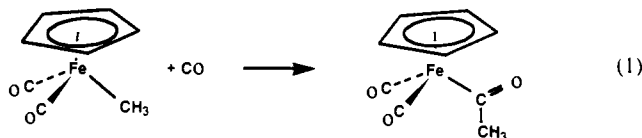
Simon T. Belt, David W. Ryba, and Peter C. Ford*

Contribution from the Department of Chemistry, University of California, Santa Barbara, California 93106. Received April 22, 1991. Revised Manuscript Received August 12, 1991

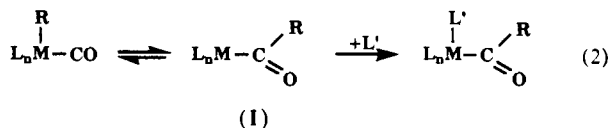
Abstract: Laser flash photolysis (308 nm) of the acyl complex $(\eta^5\text{-C}_5\text{H}_5)\text{Fe}(\text{CO})_2(\text{COCH}_3)$ leads to CO dissociation to give the intermediate $(\eta^5\text{-C}_5\text{H}_5)\text{Fe}(\text{CO})(\text{COCH}_3)$ (I') which undergoes rearrangement to give the methyl complex $(\eta^5\text{-C}_5\text{H}_5)\text{Fe}(\text{CO})_2\text{CH}_3$. Time-resolved infrared spectra suggest that I' is the solvent bound, η^1 -acyl species $(\eta^5\text{-C}_5\text{H}_5)\text{Fe}(\text{CO})\text{S}(\text{COCH}_3)$ in various solvents. Trapping of I' by CO is not competitive with the rearrangement to the methyl complex ($k_1 = 5.7 \times 10^4 \text{ s}^{-1}$ in cyclohexane) under the reaction conditions ($P_{\text{CO}} = 1 \text{ atm}$), but trapping by PPh_3 is competitive ($k_2 = 2.4 \times 10^6 \text{ L mol}^{-1} \text{ s}^{-1}$) for concentrations as small as 0.005 mol L^{-1} . Kinetics experiments show the isomerization of I' to be slower in tetrahydrofuran and acetonitrile solutions; however, the quantum yields of the transformation of $(\eta^5\text{-C}_5\text{H}_5)\text{Fe}(\text{CO})_2(\text{COCH}_3)$ to $(\eta^5\text{-C}_5\text{H}_5)\text{Fe}(\text{CO})_2\text{CH}_3$ proved to be independent of solvent and of P_{CO} .

Introduction

Carbon-carbon bond formation is a key step in homogeneously catalyzed activation of carbon monoxide in processes such as alkene hydroformylations, alcohol carbonylations, carboxylic acid homologations, reductive polymerization of CO, etc.¹ One fundamental organometallic reaction commonly invoked in proposed schemes for such catalytic cycles is the reversible "migratory insertion" of CO into a alkyl-metal bond,² e.g. Migratory in-

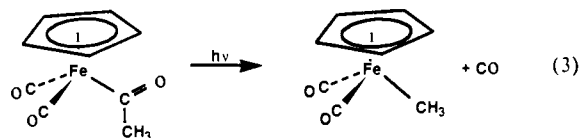


sertion mechanisms have been extensively probed via traditional (and elegant) physical-organic/physical-inorganic methods for several model compounds.³⁻⁸ Much of the attention has been focused on $\text{CH}_3\text{Mn}(\text{CO})_5$ and $\text{CpFe}(\text{CO})\text{L}(\text{CH}_3)$ (Cp = $\eta^5\text{-C}_5\text{H}_5$, L = CO or phosphine), and these studies have concluded that the rate-limiting initial step involves a methyl migration to CO via a generalized mechanism such as eq 2 rather than CO insertion into the metal-alkyl bond. However, evidence regarding the nature and kinetic behavior of the key intermediate I has remained indirect.



The reverse process of eq 1, namely the decarbonylation of metal acetyls, can often be effected using photolytic methods.⁸ Presumably, the photochemical activation results in CO labilization

to give the coordinatively unsaturated intermediate I which undergoes subsequent methyl migration to the metal center. Labeling studies have demonstrated that CO loss occurs from one of the carbonyl ligands rather than from the acetyl ligand.⁹ In this report are described the results of an investigation into the photochemical decarbonylation of $\text{CpFe}(\text{CO})_2(\text{COCH}_3)$ (eq 3) using continuous and time-resolved photolysis methods, in particular, time-resolved infrared (TRIR) techniques. These experiments provide both spectroscopic and kinetic parameters relevant to the identity and reactivity of key intermediates in the migratory insertion mechanisms of the respective metal-alkyl complex.



Experimental Section

$\text{CpFe}(\text{CO})_2(\text{COCH}_3)$, $\text{CpFe}(\text{CO})_2\text{CH}_3$, and $\text{CpFe}(\text{CO})(\text{PPh}_3)(\text{COCH}_3)$ were all synthesized using published procedures.¹⁰ Solvents for TRIR and quantum yield measurements were spectrophotometric grade (Aldrich). Alkanes and acetonitrile were distilled from CaH_2 ; tetrahydrofuran was distilled from sodium benzophenone ketal under N_2 prior to use.

Solutions for photochemical studies were prepared directly in 1-cm quartz cuvettes using serum caps to exclude air. The solvents were distilled under a nitrogen atmosphere and added to solid complexes in the cuvette, and then the resulting solutions were further deaerated by entraining with the desired gas mixture (pure N_2 or CO or mixtures of these two gases). Volumes of the solutions (3-4 mL) were then determined quantitatively by weighing the cell and its contents. Solutions were continuously stirred during photolysis experiments and were protected from spurious room light during preparations and transfers. Quantum yield measurements for the decarbonylation of $\text{CpFe}(\text{CO})_2(\text{COCH}_3)$ were carried out using a high-pressure mercury lamp with a 313-nm interference filter as the excitation source (typical intensity 4×10^{-7} einsteins/L s) on an optical train described previously.¹¹ Ferrioxalate actinometry was used to determine photolysis light intensities, and changes in the concentrations of reactants and products were determined from changes in UV-visible spectra recorded on a Hewlett-Packard diode array spectrometer (8452A) or IR spectra obtained with a Bio-Rad FTS-60 FTIR interferometer.

(1) Henríci-Olivé, G.; Olivé, S. *Catalyzed Hydrogenation of Carbon Monoxide*; Springer-Verlag, Berlin, 1984.

(2) Collman, J. P.; Hegedus, L. S.; Norton, J. R.; Finke, R. G. *Principles and Applications of Organotransition Metal Chemistry*; University Science Books: 1987; Chapter 6.

(3) Wojcicki, A. *Adv. Organomet. Chem.* **1973**, *11*, 87-145.

(4) Calderazzo, F. *Angew. Chem., Int. Ed. Engl.* **1977**, *16*, 299-311.

(5) (a) Flood, T. C. *Top. Stereochem.* **1981**, *12*, 37-118. (b) Flood, T. C.; Jensen, J. E.; Statler, J. A. *J. Am. Chem. Soc.* **1981**, *103*, 4410.

(6) Butler, I.; Basolo, F.; Pearson, R. G. *Inorg. Chem.* **1967**, *6*, 2074.

(7) (a) Cawse, J.; Fiato, R. A.; Pruet, R. J. *Organomet. Chem.* **1979**, *172*, 405. (b) Webb, S.; Giandomenico, C.; Halpern, J. *J. Am. Chem. Soc.* **1986**, *108*, 345.

(8) King, R. B.; Bisnette, M. B. *J. Organomet. Chem.* **1964**, *2*, 15-37.

(9) McHugh, T. M.; Rest, A. J. *J. Chem. Soc., Dalton Trans.* **1980**, 2323-2332.

(10) (a) Eisch, J. J.; King, R. B. *Organometallic Syntheses*; Academic Press: New York, 1965; Vol. 1, p 151. (b) Treichel, P. M.; Shubkin, R. L.; Barnett, K. W.; Reichard, D. *Inorg. Chem.* **1966**, *5*, 1177-1181.

(11) (a) Hintze, R. D.; Ford, P. C. *J. Am. Chem. Soc.* **1975**, *97*, 2664-2671. (b) Desrosiers, M. F.; Wink, D. A.; Trautman, R.; Friedman, A. E.; Ford, P. C. *J. Am. Chem. Soc.* **1986**, *108*, 1917-1927.

Table I. Spectral Data for Reactants and Products

compound	solvent ^a	λ_{max} (ϵ , $\text{M}^{-1} \text{cm}^{-1}$)	ν_{CO} (ϵ , $\text{M}^{-1} \text{cm}^{-1}$)
$(\eta^5\text{-C}_5\text{H}_5)\text{Fe}(\text{CO})_2(\text{COCH}_3)$	hexane	334 (4.65×10^3)	2020 (2.6×10^3) 1965 (5.2×10^3) 1670 (1.34×10^3)
	c-C ₆ H ₁₂	334 (4.65×10^3)	2018, 1963, 1669
	isooctane	334 (4.65×10^3)	2018, 1962, 1670
	THF	328 (4.55×10^3)	2015, 1955, 1658
	CH ₃ CN	322 (4.34×10^3)	2018, 1958, 1650
$(\eta^5\text{-C}_5\text{H}_5)\text{Fe}(\text{CO})_2\text{CH}_3$	Xe (1) ^b		2025, 2019, 1965, 1673
	n-hexane	351 (9.9×10^2)	2014 (7.0×10^3), 1961 (8.1×10^3)
	c-C ₆ H ₁₂	351 (9.9×10^2)	2013, 1960
	isooctane	351 (9.9×10^2)	2012, 1958
	THF	350 (10.0×10^2)	2010, 1952
$(\eta^5\text{-C}_5\text{H}_5)\text{Fe}(\text{CO})(\text{COCH}_3)$	CH ₃ CN	350 (10.0×10^2)	2004, 1943
	n-hexane		1949
	cyclohexane		1949
	isooctane		1949
	THF		1921
$(\eta^5\text{-C}_5\text{H}_5)\text{Fe}(\text{CO})(\text{PPh}_3)\text{COCH}_3$	CH ₃ CN		1926
	Xe (1) ^b		1938, 1582
	hexane		1924 (4.1×10^3) 1612 (~ 400)

^a Room temperature solutions except where noted. ^b 193 K, see ref 19.

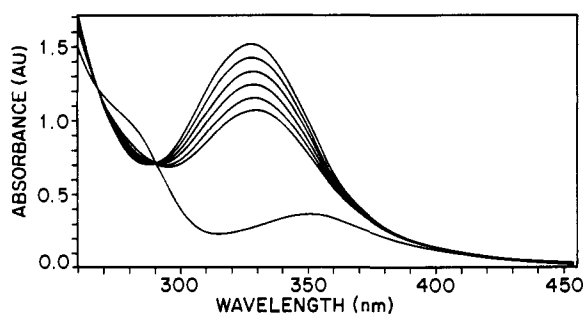


Figure 1. Sequential spectra recorded during the 313-nm photolysis of $(\eta^5\text{-C}_5\text{H}_5)\text{Fe}(\text{CO})_2(\text{COCH}_3)$ ($3.3 \times 10^{-4} \text{ mol L}^{-1}$) in a dinitrogen purged THF solution. Trace with highest absorbance at 328 nm is the initial spectrum; final trace is $(\eta^5\text{-C}_5\text{H}_5)\text{Fe}(\text{CO})_2\text{CH}_3$.

The flash photolysis apparatus used for TRIR experiments has been described in detail elsewhere.¹² Solutions prepared as above and under the desired gas mixtures were passed through the photolysis cells using a simple flow apparatus which allowed for multiple pulse data collection and averaging experiments.¹² The photolysis cell consisted of a modified McCarthy IR cell with CaF₂ windows and a 1.0-mm Teflon spacer. Stainless steel cannula were silver-soldered to the brass cell body for transfer of solutions into and from the reservoirs of the flow apparatus. Laser excitation of 308 nm was accomplished with a Lambda Physik Model LPX 105 XeCl excimer laser. The detection system consisted of a Spectra Physics/Laser Analytics Model SP5800 lead salt diode IR laser probe source, tunable over the approximate frequency range 1600–2200 cm^{-1} and a Santa Barbara Research Center PV Hg/Cd/Te fast risetime IR detector. Details of the optical train and the data manipulation have been published.^{12a}

Results

Continuous Photolysis Studies. In agreement with previous reports,^{8,13} the photolysis of $\text{CpFe}(\text{CO})_2(\text{COCH}_3)$ (A, λ_{max} (in alkanes) = 334 nm, Table I) was demonstrated to lead cleanly to the formation of $\text{CpFe}(\text{CO})_2\text{CH}_3$ (B, 352 nm) in various solvents both in the presence and the absence of added CO. The UV-visible spectral changes accompanying the 313-nm irradiation of A in THF under N₂ are shown in Figure 1. The observation of isosbestic points at 269 and 291 nm indicates a single photochemical process with no significant formation of additional species such as the dimer $[\text{CpFe}(\text{CO})_2]_2$.¹⁴ The quantum yield for

Table II. Quantum Yields and Rate Constants for the 313-nm Continuous Photolysis of $(\eta^5\text{-C}_5\text{H}_5)\text{Fe}(\text{CO})_2(\text{COCH}_3)$ in Various Solvents

solvent	atm	Φ_{313}^a	k_1^b (s^{-1})
cyclohexane	Ar	0.64 ± 0.02	5.7×10^4
	CO	0.64 ± 0.02	5.7×10^4
isooctane	Ar	0.64 ± 0.02	4.0×10^4
	CO	0.64 ± 0.02	4.0×10^4
hexane	Ar	0.64 ± 0.02	4.0×10^4
	CO	0.64 ± 0.02	4.0×10^4
THF	Ar	0.62 ± 0.04	1.3×10^4
	CO	0.62 ± 0.04	1.3×10^4
CH ₃ CN	Ar	0.62 ± 0.04	<1.0
	CO	0.62 ± 0.04	<1.0

^a Quantum yield for continuous wave photolysis; experimental uncertainties are calculated for five or more duplicate runs. ^b First-order rate constant for disappearance of the intermediate 1'. Experimental uncertainties are estimated conservatively at $\pm 10\%$ based upon five or more duplicate runs.

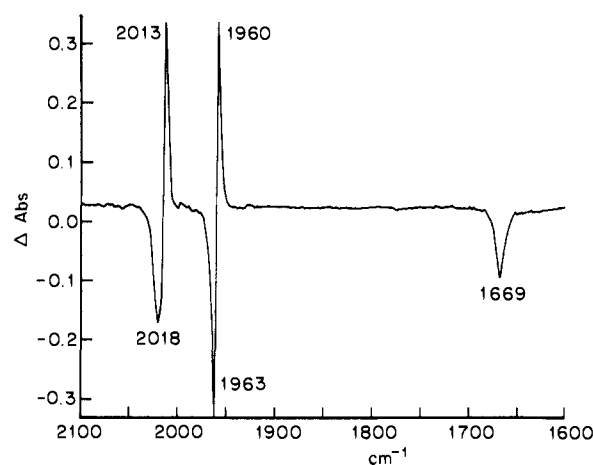


Figure 2. FTIR difference spectrum of a cyclohexane solution of $(\eta^5\text{-C}_5\text{H}_5)\text{Fe}(\text{CO})_2(\text{COCH}_3)$ ($3 \times 10^{-3} \text{ M}$) showing 308-nm laser photolysis induced loss of parent compound and production of $(\eta^5\text{-C}_5\text{H}_5)\text{Fe}(\text{CO})_2\text{CH}_3$.

decarbonylation (Φ_d , eq 3) was determined to be 0.62 ± 0.02 mol/einstein in THF under dinitrogen. The same Φ_d was found for photolysis under various P_{CO} up to 1 atm, a result which indicated the unimportance of back reaction between the presumed intermediate $\text{CpFe}(\text{CO})(\text{COCH}_3)$ (see below) and CO under these conditions. In other solvents, including cyclohexane and acetonitrile, Φ_d proved to be insensitive to the nature of the solvent as

(12) (a) DiBenedetto, J. A.; Ryba, D. W.; Ford, P. C. *Inorg. Chem.* **1989**, *28*, 3503–3507. (b) Belt, S. T.; Ryba, D. W.; Ford, P. C. *Inorg. Chem.* **1990**, *29*, 3633–3634.

(13) Alexander, J. J. *J. Am. Chem. Soc.* **1975**, *97*, 1729–1732.

(14) Kazlauskas, R. J.; Wrighton, M. S. *Organometallics* **1982**, *1*, 602–611.

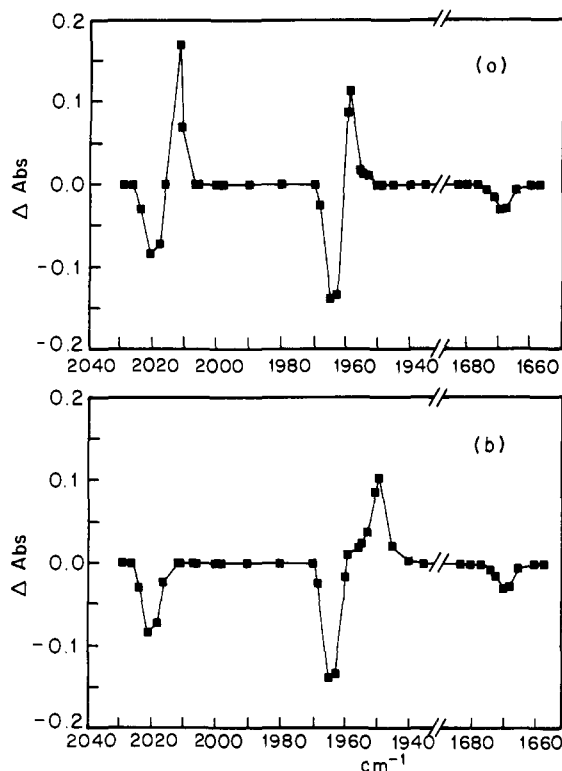


Figure 3. (a) Transient difference spectrum of $(\eta^5\text{-C}_5\text{H}_5)\text{Fe}(\text{CO})_2(\text{COCH}_3)$ in cyclohexane taken 100 μs after 308-nm laser pulse. (b) Transient difference spectrum of $(\eta^5\text{-C}_5\text{H}_5)\text{Fe}(\text{CO})_2(\text{COCH}_3)$ in cyclohexane taken 1 μs after 308-nm laser pulse.

well as independent of P_{CO} (Table II).

The photochemical decarbonylation of $\text{CpFe}(\text{CO})_2(\text{COCH}_3)$ was also investigated using FTIR. Figure 2 illustrates an FTIR difference spectrum following 308-nm excitation of **A** in C_6H_{12} under Ar. The negative absorbance changes at ν_{CO} 2018, 1963 (metal carbonyl), and 1669 cm^{-1} (acetyl) correspond to the depletion of **A**, while the positive changes at 2013 and 1960 cm^{-1} correspond to the formation of **B**. Similar IR changes were observed in THF and CH_3CN solutions (see Table I).

Flash Photolysis of $\text{CpFe}(\text{CO})_2(\text{COCH}_3)$ in Cyclohexane Using TRIR Detection. Laser flash photolysis (308 nm) **A** in cyclohexane solution (10^{-3} mol L^{-1}) under Ar was shown to lead to the rapid and permanent depletion of the parent compound as monitored by TRIR detection at the high-frequency side of the metal carbonyl absorption bands (i.e., 2021 and 1965 cm^{-1}). Depletion of **A** was also observable via the acetyl mode at 1669 cm^{-1} . At the monitoring frequencies to lower energy from either 2021 or 1965 cm^{-1} , the absorbance changes resulting from the depletion of **A** became smaller, and a new species was observed to grow in over a period of ~ 100 μs . The maximum absorbance changes of this new species appear at 2012 and 1959 cm^{-1} which are indicative of the formation of the final product, $\text{CpFe}(\text{CO})_2\text{CH}_3$. The TRIR spectrum obtained 100 μs after the laser flash is illustrated in Figure 3a and shows excellent agreement with the difference FTIR spectrum displayed in Figure 2. On a shorter time scale (i.e., 1 μs following the flash), the TRIR difference spectrum showed only the transient metal carbonyl absorbance at 1949 cm^{-1} (Figure 3b) and none of the absorptions attributable to **B**. The position of the 1949- cm^{-1} band is in close agreement with that found for the purported intermediate $\text{CpFe}(\text{CO})(\text{COCH}_3)$ ($\nu_{\text{CO}} = 1948$ cm^{-1}) produced by photolysis of **A** in a methane matrix at 12 K.¹⁵

The disappearance of the transient absorbance at 1949 cm^{-1} (Figure 3b) followed first-order kinetics with a half-life of ca. 20 μs . The rate constant determined for the decay of this intermediate

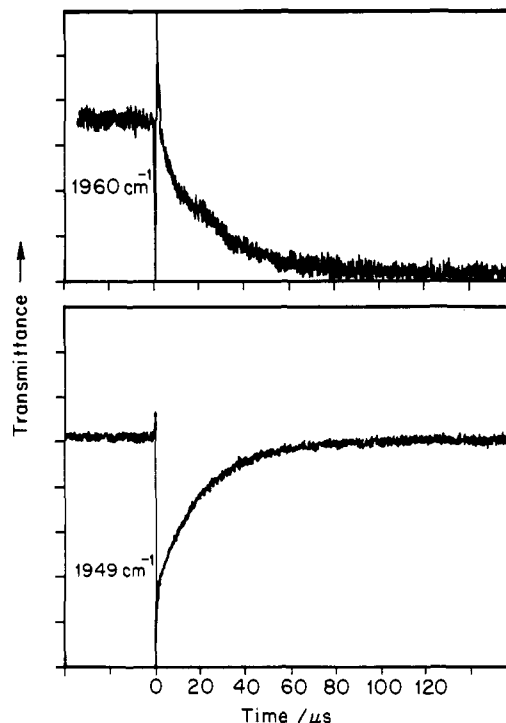


Figure 4. Temporal transmittance of dinitrogen purged cyclohexane solution of $(\eta^5\text{-C}_5\text{H}_5)\text{Fe}(\text{CO})_2(\text{COCH}_3)$: (upper) monitored at 1960 cm^{-1} showing growth of product and (lower) monitored at 1949 cm^{-1} showing the loss of intermediate.

(*I'*), $k_{\text{obs}} = 5.7 \times 10^4$ s^{-1} , proved to be identical to that for formation of **B** as measured at either 2010 or 1958 cm^{-1} (Figure 4). Furthermore, the rate of decay of *I'* was found to be independent of P_{CO} , consistent with the observation above that the overall quantum yields for photodecarbonylation of **A** were also insensitive to P_{CO} . These results imply that *I'* is not measurably trapped by added CO in competition with methyl migration to the metal center under these conditions.

In contrast, when photolyses of $\text{CpFe}(\text{CO})_2(\text{COCH}_3)$ were carried out in the presence of added PPh_3 , the phosphine complex $\text{CpFe}(\text{CO})\text{PPh}_3(\text{COCH}_3)$ ($\nu_{\text{CO}} = 1924$ cm^{-1}) was also formed as one product of the photoreaction, in agreement with a previous, qualitative report.¹³ In addition, the decay of the intermediate *I'* was accelerated under these conditions. A plot of k_{obs} (the rate constant for the first order decay of *I'*) vs $[\text{PPh}_3]$ proved to be linear (slope = 2.4×10^6 $\text{L mol}^{-1} \text{s}^{-1}$) with a nonzero intercept (5.6×10^4 s^{-1}) (Figure 5).

Photolysis of $\text{CpFe}(\text{CO})_2(\text{COCH}_3)$ in Different Solvents. Laser flash photolysis of **A** in *n*-heptane or isooctane under Ar or CO resulted in the formation of transient species whose ν_{CO} modes and rates of reaction are close to those found for cyclohexane solution (see Table II). In freshly distilled THF, laser photolysis of **A** resulted in the formation of a transient species which displayed a single metal carbonyl mode at 1921 cm^{-1} in the TRIR and decayed via first-order kinetics, $k_1 = 1.3 \times 10^4$ s^{-1} . Once again, the decay of this intermediate was accompanied by the formation of $\text{CpFe}(\text{CO})_2\text{CH}_3$ as shown by ν_{CO} maxima at 2010 and 1952 cm^{-1} . When water (~ 0.1 mol L^{-1}) was added to the THF solvent, the rate of decay of the intermediate as monitored at 1921 cm^{-1} was observed qualitatively to decrease by about two orders of magnitude. Furthermore, when CH_3CN was used as solvent, an intermediate was formed which had a broad ν_{CO} mode centered at 1926 cm^{-1} having a lifetime in excess of 1 ms. A difference FTIR spectrum recorded several minutes following irradiation revealed that the intermediate had indeed isomerized to form **B** as observed in all other solvents. In accord with the spectral observations in alkane solutions, the acetyl ν_{CO} absorption of *I'* was not detected by the TRIR technique in either THF or CH_3CN solution. The ν_{CO} frequencies for **A**, **B**, and the intermediate *I'* in different solvents are summarized in Table I. In

(15) (a) Fettes, D. J.; Narayanaswamy, R.; Rest, A. J. *J. Chem. Soc., Dalton Trans.* **1981**, 2311–2316. (b) Hitam, R. B.; Narayanaswamy, R.; Rest, A. J. *J. Chem. Soc., Dalton Trans.* **1983**, 615–619.

Scheme 1

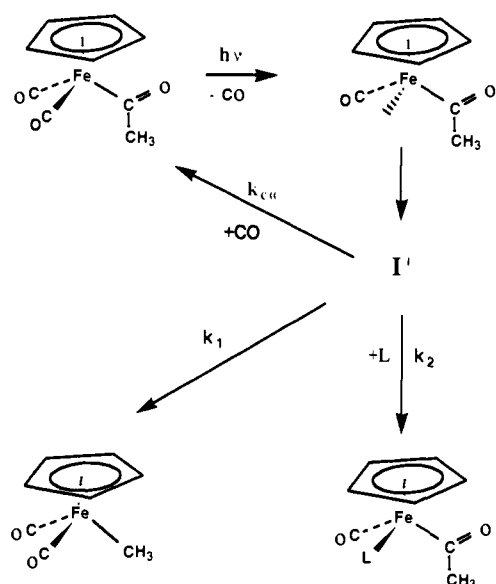


Table II are summarized the quantum yield and kinetics data.

Discussion

The above results demonstrate that UV excitation of $\text{CpFe}(\text{CO})_2(\text{COCH}_3)$ in a range of solvents leads to CO loss and gives a reactive intermediate (I') whose kinetics and spectroscopic properties have been observed directly using TRIR methods. In the absence of added substrates, I' undergoes a rapid rearrangement to give the metal alkyl $\text{CpFe}(\text{CO})_2\text{CH}_3$ via first-order kinetics (eq 4). This intermediate does not react noticeably with

$$\frac{dB}{dt} = -\frac{dI'}{dt} = k_{\text{obs}}[I'] \quad (4)$$

CO in a solution under $P_{\text{CO}} = 1$ atm ($[\text{CO}] \sim 0.01$ mol L^{-1}), but it does react measurably with PPh_3 at concentrations as low as 0.005 mol L^{-1} to give the substitution product of $\text{CpFe}(\text{CO})(\text{PPh}_3)(\text{COCH}_3)$ in competition with formation of **B**. These observations can be interpreted in terms of the pathways described in Scheme 1 in which CO photodissociation from **A** leads to the formation of the intermediate I' which can decay via several competing pathways, methyl migration to the iron center (k_1), trapping by CO to reform starting material (k_{CO}), and trapping by another ligand **L** to give the substitution product $\text{CpFe}(\text{CO})\text{L}(\text{COCH}_3)$ (k_2). Accordingly, the rate constant k_{obs} for the disappearance of I' can be rewritten as

$$k_{\text{obs}} = k_1 + k_{\text{CO}}[\text{CO}] + k_L[\text{L}] \quad (5)$$

The CO independence both of the quantum yield for the decarbonylation of **A** and of the I' decay rate leads one to conclude that, for the conditions investigated, the value of k_{CO} must be sufficiently small that $k_1 \gg k_{\text{CO}}[\text{CO}]$. Since the maximum $[\text{CO}]$ investigated was about 0.01 mol L^{-1} , an experimental uncertainty of $\pm 10\%$ in the k_{obs} values would lead to an upper limit of $\sim 6 \times 10^5$ L mol $^{-1}$ s $^{-1}$ for the reaction of CO with I' in cyclohexane an upper limit of $\sim 1 \times 10^5$ L mol $^{-1}$ s $^{-1}$ for this reaction in THF. The relative inability of CO to compete with alkyl migration in an intermediate analogous to I' was also concluded by Flood and Campbell¹⁶ based on a steady-state kinetics analysis of the rates of carbonylation of a similar iron-alkyl complex.

When triphenylphosphine was present in cyclohexane solutions of **A**, ligand photosubstitution to give $\text{CpFe}(\text{CO})(\text{PPh}_3)\text{L}(\text{COCH}_3)$ was observed to be competitive with alkyl migration. The linear plot of Figure 5 is consistent with the relationship $k_{\text{obs}} = k_1 + k_2[\text{PPh}_3]$ with the intercept (5.6×10^4 s $^{-1}$) equal to k_1 and the slope (2.4×10^6 L mol $^{-1}$ s $^{-1}$) equal to k_2 . Notably, k_2 is sub-

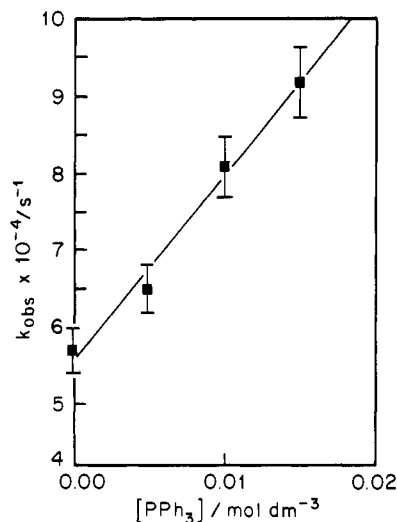
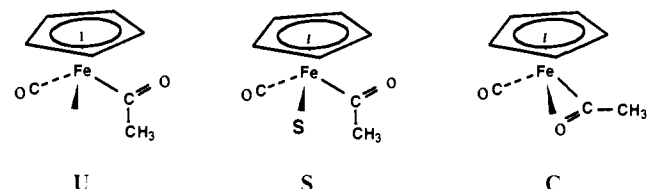


Figure 5. Plot of k_{obs} vs $[\text{PPh}_3]$. Rates are calculated from the temporal absorbance at 1949 cm^{-1} following 308-nm XeCl excimer laser photolysis of $(\eta^5\text{-C}_5\text{H}_5)\text{Fe}(\text{CO})_2(\text{COCH}_3)$ (10^{-3} mol L^{-1} in dinitrogen purged cyclohexane).

stantially larger than the upper limit of k_{CO} . Although the analogy is rather distant, it is notable that the flash photolysis generated intermediate $\text{Cp}_2\text{Fe}_2(\text{CO})_3$ has been shown to react with CO with a rate constant about a factor of 3 slower than that for PPh_3 .¹⁷

In the above discussion, the general formula for I' has been assigned as $\text{CpFe}(\text{CO})(\text{COCH}_3)$; however, several different configurations illustrated below come to mind as possible structures of this species. The truly unsaturated structure **U** must be



considered very unlikely, given strong evidence that, even in hydrocarbon solutions, the empty site of pentacoordinate d^6 metal carbonyls generated by photolytic dissociation of CO is coordinated by solvent within a few picoseconds.¹⁸ On the other hand, the C-H bond of the methyl group could coordinate to the metal to give an "agostic" interaction which would be difficult to differentiate via IR spectroscopy from a hydrocarbon solvent molecule occupying the same site. Indeed the agostic configuration would appear closer to the transition state one might propose for methyl migration to the metal center than would either the solvated form **S** and the η^2 "chelated" acyl structure **C**. Theoretical calculations have concluded that for the $\text{Mn}(\text{CO})_4(\text{C}(\text{O})\text{CH}_3)$ fragment, the η^2 -carbonyl is much more stable than the unsaturated analogue of **U**;¹⁹ neither the solvated or agostic configurations were considered in these studies.

Distinguishing between the above possible structures of I' requires a closer examination of the solvent dependence on the experimental spectroscopic and kinetic properties of this species. In principle, one would expect the reaction kinetics and IR spectra of an agostic bound version of **U** and the η^2 -acyl structure **C** to be less sensitive to the nature of the solvent than would be the η^1 -acetyl structure type **S**, where there is a direct interaction

(17) (a) Dixon, A. J.; Healy, M. A.; Hodges, P. M.; Moore, B. D.; Poliakoff, M.; Simpson, M. B.; Turner, J. J.; West, M. J. *J. Chem. Soc., Faraday Trans. 2* **1986**, *82*, 2083-2092. (b) Another distantly related example is the intermediate $\text{CpFe}(\text{CO})(\eta^3\text{-CH}_2\text{Ph})$ which reacts 9-fold faster with PPh_3 than with CO.^{17c} (c) Herrick, R. S.; Frederick, A. B.; Duff, R. R. *Organometallics* **1989**, *8*, 1120-1121.

(18) (a) Joly, A. G.; Nelson, K. A. *J. Phys. Chem.* **1989**, *93*, 2876-2878. (b) Lee, M.; Harris, C. B. *J. Am. Chem. Soc.* **1989**, *111*, 8963-8965.

(19) Ziegler, T.; Verluis, L.; Tscinke, V. *J. Am. Chem. Soc.* **1986**, *108*, 612-617.

(16) Flood, T. C.; Campbell, K. D. *J. Am. Chem. Soc.* **1984**, *106*, 2853-2860.

between the solvent and the metal center. For **S**, it would be expected that the rate of methyl migration to the metal would be slowed and that the frequency of the metal carbonyl ν_{CO} band would be shifted to lower values as the donor strength of the solvent is increased. The latter prediction is certainly consistent with the observations (Table I) that upon changing the solvent from hydrocarbons to THF, the position of the ν_{CO} mode for $\text{CpFe}(\text{CO})(\text{COCH}_3)$ shifted 26 cm^{-1} to lower frequency (from 1949 to 1923 cm^{-1}). The corresponding absorption band in CH_3CN is extremely broad compared with alkane or THF solutions but is centered at a significantly lower frequency (1926 cm^{-1}) than that found in alkanes. However, the rate constant for alkyl migration (k_1 , Table II) is only a factor of 4 lower in THF than in cyclohexane, heptane, or isooctane, although, when acetonitrile was employed as the solvent, alkyl migration proved to be too slow to allow direct monitoring with the present detection system. The greater effect of acetonitrile may be the result of a significantly stronger coordination of CH_3CN to the CpFe fragment.²⁰ It is our conclusion that if a single structure is appropriate to describe **I'** the solvated species **S** with the η^1 -acyl configuration is the more consistent with the above observations. It is certainly possible that configuration **U**(agostic) or **C** is present in hydrocarbon solutions, while **S** is the dominant species in more strongly donating solvents; however, the observation that, even in liquid xenon, **I'** has a significantly lower frequency ν_{CO} than in hydrocarbons (Table I)²¹ argues for the presence of an **S** configuration even in this solvent.

Further verification for this structure might come from IR spectral observation of the acetyl ν_{CO} mode of **I'** in addition to the terminal metal carbonyl ν_{CO} values listed in Table I. At present, two explanations may account for the failure to observe this band by TRIR. If the frequency of the acetyl ν_{CO} were $<1550\text{ cm}^{-1}$, it would lie outside of the range of the detection frequency limits of the current instrument. This would represent a shift of more than 120 cm^{-1} to lower frequency from that observed for

the acyl ν_{CO} of **A**. Alternatively, the acetyl mode may possess a reduced intensity compared to the parent vibration and therefore remain undetected. For the Fe complexes under study here, the ratio in intensity of the acetyl mode to the most intense of the terminal carbonyl modes in $\text{CpFe}(\text{CO})_2(\text{COCH}_3)$ is 1:4. A similar ratio for **I'** would allow straightforward detection of the acetyl mode given the absorbance change due to depletion of $\text{CpFe}(\text{CO})_2(\text{COCH}_3)$ following irradiation; however, it is notable that the analogous intensity ratios for the monocarbonyl complexes $\text{CpFe}(\text{CO})(\text{PPh}_3)(\text{COCH}_3)$ and $\text{CpFe}(\text{CO})(\text{Xe})(\text{COCH}_3)$ ²¹ are factors of 3 and 8, respectively, smaller. Thus for $\text{CpFe}(\text{CO})(\text{COCH}_3)$, the absorbance change in the 1600-cm^{-1} region may be too small to allow detection within the TRIR instrument's signal-to-noise limits. However, it should be noted that low acyl ν_{CO} band intensity has been used to argue for η^2 -acyl coordination in intermediates formed in the low-temperature matrix photolysis of $(\text{CH}_3\text{CO})\text{Co}(\text{CO})_4$.²²

In summary, the laser flash photolysis experiments described here have allowed the detection and characterization of the reaction kinetics of the short-lived ($<100\text{ }\mu\text{s}$ in ambient temperature hydrocarbon solutions) species $\text{CpFe}(\text{CO})(\text{COCH}_3)$, the proposed intermediate in the migratory insertion reaction 1. Under $P_{\text{CO}} = 1\text{ atm}$, the reaction of **I'** is not competitive with methyl migration to the metal center. Trapping of **I'** by PPh_3 is more efficient. The solvent effect on observed ν_{CO} frequencies in the time-resolved infrared spectra in a variety of solvents points to **I'** being the solvated complex $(\eta^5\text{-C}_5\text{H}_5)\text{Fe}(\text{CO})\text{S}(\eta^1\text{-COCH}_3)$.

Acknowledgment. This research was sponsored by a grant (DE-FG03-85ER13317) from the Division of Chemical Sciences, Office of Basic Energy Sciences, U.S. Department of Energy. The instrumentation used was constructed from components purchased with funds from the National Science Foundation (CHE-87-22561 and CHE-84-113020), the UCSB Faculty Research Committee and the UCSB Quantum Institute and from components donated by the Newport Corporation and the Amoco Technology Co. S.T.B. acknowledges support from a NATO Fellowship awarded through the SERC (UK).

Registry No. $\text{CpFe}(\text{CO})_2(\text{COCH}_3)$, 12108-22-4; $\text{CpFe}(\text{CO})_2\text{CH}_3$, 12080-06-7; $\text{CpFe}(\text{CO})\text{PPh}_3(\text{COCH}_3)$, 12101-02-9; $(\eta^5\text{-C}_5\text{H}_5)\text{Fe}(\text{CO})(\text{COCH}_3)$, 81448-76-2; $(\eta^5\text{-C}_5\text{H}_5)\text{Fe}(\text{CO})(\text{COCH}_3)(\text{THF})$, 136947-54-1; $(\eta^5\text{-C}_5\text{H}_5)\text{Fe}(\text{CO})(\text{COCH}_3)(\text{CH}_3\text{CN})$, 83006-09-1.

(20) Gill, T. P.; Mann, K. R. *Inorg. Chem.* **1983**, *22*, 1986-1991.

(21) (a) Since the TRIR experiment was unable to detect the expected acyl carbonyl frequency of **I'** in ambient temperature solution over the range $1680\text{-}1550\text{ cm}^{-1}$ despite clear observation of the terminal ν_{CO} mode, preliminary experiments were carried out to examine the IR spectra of intermediates in the analogous flash photolysis of **A** in liquid Xe (193 K).^{19b} A weak acyl band at 1582 cm^{-1} was detected using FTIR methods (the terminal carbonyl ν_{CO} was detected at 1938 cm^{-1}). (b) Experiments carried out by Belt, S. T.; Ryba, D. W.; Kyle, K. R. in the laboratories of Bergman, R. G. and Moore, C. B. at the University of California, Berkeley.

(22) Sweany, R. L. *Organometallics* **1989**, *8*, 175-179.